

# Ab Initio Theoretical Studies of the Rydberg States of Formaldehyde<sup>1</sup>

Lawrence B. Harding and William A. Goddard III\*

*Contribution No. 5368 from the Arthur Amos Noyes Laboratory of Chemical Physics, California Institute of Technology, Pasadena, California 91125.*

*Received June 25, 1976*

**Abstract:** Ab initio configuration interaction (GVB-CI) methods are used to study the excited Rydberg states of formaldehyde formed by exciting out of either the  $n$  or  $\pi$  orbital into the various 3s, 3p, and 3d-like Rydberg orbitals. The resulting excitation energies are in good agreement (within  $\sim 0.1$  eV) with the available experimental results. Calculated oscillator strengths are in fair agreement with experiment. Two states  $^1(\pi \rightarrow \pi^*)$  and  $^1(\pi \rightarrow 3s)$  are calculated to lie between 10.7 and 10.8 eV, corresponding closely to a broad unassigned peak in the electron impact spectrum (10.5–11.0 eV). We have assigned other peaks in the electron impact spectrum at 11.4–12.0 eV and 12.5–12.8 eV as resulting from  $(\pi \rightarrow 3p)$  and  $(\pi \rightarrow 3d)$  transitions, respectively.

## I. Introduction

The electronic states of simple organic molecules can be categorized according to size as either valence or Rydberg. In a previous paper<sup>2</sup> we reported the results of ab initio generalized valence bond (GVB) calculations on the valence states of formaldehyde,  $^3,^1(n \rightarrow \pi^*)$  and  $^3(\pi \rightarrow \pi^*)$ . It is the purpose of this paper to extend this treatment to the Rydberg states.

The Rydberg states of formaldehyde have been the subject of numerous recent experimental<sup>3-9</sup> and theoretical<sup>9-15</sup> investigations. Experimentally, dipole-allowed  $n \rightarrow s$ ,  $n \rightarrow p$ , and  $n \rightarrow d$  Rydberg series have been assigned in both the optical and electron impact spectra. However, there has been no conclusive assignment of a Rydberg state resulting from excitation out of the  $\pi$  orbital (we denote such states as  $\pi$  Rydberg) in either the optical or electron impact spectra. In

fact, no peaks are found in the photoabsorption spectrum of formaldehyde in the 10.5–13 eV region where the  $n = 3$  members of the  $\pi$  Rydberg series are expected. Although poorly resolved peaks are found in this region of the electron impact spectrum, they have not yet been assigned.

Previous theoretical studies of the formaldehyde Rydberg states have been limited either by the number of states considered or the accuracy of the computational method used. Calculations using correlated wave functions have been reported<sup>10,11,14</sup> on the  $n \rightarrow 3s$ ,  $n \rightarrow 3p$ ,  $\pi \rightarrow 3s$ , and  $\pi \rightarrow 3p_z$  states. In addition, single configuration calculations<sup>9</sup> have been reported on some of the  $n \rightarrow 3d$  and  $\pi \rightarrow 3d$  states. In this paper we report the results of extensive ab initio calculations on all the  $n = 3$  Rydberg states associated with the first two ionization potentials of formaldehyde.

The details of the calculational method are discussed in section II, the results are presented and discussed in section III, and a detailed discussion of the  $^1(\pi \rightarrow \pi^*)$  state is contained in section IV.

## II. Calculational Details

**A. Basis Sets and Geometry.** The double  $\zeta$  (DZ) basis set of Huzinaga<sup>16</sup> and Dunning<sup>17</sup> augmented with a set of d basis functions ( $\zeta_c = 0.6769$ ,  $\zeta_o = 0.8853$ ) was used for the ground and ion state calculations. For calculations on Rydberg states, this basis was augmented with two sets each of diffuse s ( $\zeta_c = 0.023$ ,  $\zeta_o = 0.032$ ), p ( $\zeta_c = 0.021$ ,  $\zeta_o = 0.028$ ), and d ( $\zeta_c = \zeta_o = 0.015$ ) primitive Gaussians. The exponents of the diffuse functions are those of Dunning,<sup>18</sup> optimized for atomic Rydberg calculations. In addition, to test the completeness of our diffuse d basis, a second set of calculations was carried out on some states using the same diffuse s and p functions but with two sets of diffuse d functions, the exponents and contraction coefficients of which are shown in Table I.

The experimental ground state geometry,<sup>19</sup>  $R_{CO} = 1.2099$  Å,  $R_{CH} = 1.1199$  Å,  $\angle HCH = 118^\circ$ , was used for all calculations.

**B. Calculational Method.** The perfect-pairing GVB method<sup>20</sup> has been described in detail elsewhere. Briefly we define our notation as follows: a GVB( $p/q/PP$ ) closed shell singlet wave function can be written

$$\mathcal{A} \left\{ \left[ \prod_{i=1}^k \phi_i^2 \right] \left[ \prod_{i=1}^p (\lambda_{ai} \phi_{ai}^2 - \lambda_{bi} \phi_{bi}^2 - \lambda_{ci} \phi_{ci}^2 \dots) \right] \alpha \beta \alpha \beta \dots \alpha \beta \right\} \quad (1)$$

where  $q$  is defined to be the total number of orbitals involved in the second product (i.e., all orbitals with occupancy,  $2\lambda^2$ , less than two). Similarly, the corresponding GVB( $p/q/PP$ ) open-shell singlet or triplet wave function can be written, as in (2),

$$\mathcal{A} \left\{ \left[ \prod_{i=1}^k \phi_i^2 \right] \left[ \prod_{i=1}^{p-2} (\lambda_{ai} \phi_{ai}^2 - \lambda_{bi} \phi_{bi}^2 \dots) \right] \times (\phi_{p-1} \phi_p \pm \phi_p \phi_{p-1}) \alpha \beta \dots \alpha \beta \mp \beta \alpha \right\} \quad (2)$$

Under the perfect-pairing restriction, all of the orbitals are taken to be orthogonal and the spin function is taken as indicated. Thus the GVB wave functions consist of a core of electron pairs described with doubly occupied orbitals together with a set of correlated pairs each described by a dominant or bonding natural orbital (NO) and a variable number of correlating NO's. All orbitals and occupation numbers,  $\lambda$ , are solved for self-consistently.<sup>21</sup>

It has been found that the GVB orbitals form an effective basis for relatively small configuration interaction (CI) calculations which both relax the perfect-pairing restriction and

**Table I.** Exponents and Contraction Coefficients for Diffuse d Functions<sup>a</sup>

| Carbon    |              | Oxygen   |             |
|-----------|--------------|----------|-------------|
| Exponents | Coefficients | Exponent | Coefficient |
| 0.2556    | 0.021 75     | 0.2951   | 0.030 61    |
| 0.0752    | 0.108 96     | 0.0984   | 0.143 7     |
| 0.0250    | 0.926 16     | 0.0328   | 0.898 7     |
| 0.0083    | 1.000        | 0.0109   | 1.000       |

<sup>a</sup> The first three of each type are contracted together with the coefficients given.

include important correlation effects neglected in the GVB wave functions.

Consider now formaldehyde as an example to elucidate further the nature of GVB wave functions. It was found previously<sup>2</sup> that for the purpose of calculating valence excitation energies very small CI calculations using the GVB(2/4) orbitals (correlating only the CO  $\sigma$  and  $\pi$  pairs with one correlating NO/pair) are sufficient. Calculations of this accuracy lead to  $n \rightarrow \pi^*$  and  $^3(\pi \rightarrow \pi^*)$  excitation energies within 0.1 eV of the experimental values. Unfortunately, calculations at the GVB(2/4)-CI level of accuracy lead to ionization potentials that are 0.7 to 1.0 eV below the experimental results.<sup>22</sup> Since Rydberg states involve excitations to orbitals which are large with respect to the molecule, it is expected that calculational methods which yield inaccurate ionization potentials will yield equally inaccurate Rydberg excitation energies.

The error is basically due to a differential correlation effect; that is, the neglected correlation energy of the ground state is greater than the neglected correlation energy of the Rydberg or ion states and hence the calculated excitation energies are too low. In order to correct this error it is necessary either to correct empirically the uncorrelated energies or to use a more accurate wave function in which the important differential correlation effects are included. We have chosen the latter option.

The calculations reported here are based on GVB(5/14/PP) wave functions. Taking the ground state as an example, the GVB(5/14/PP) wave function can be written,

$$\mathcal{A} \{ \phi_{1sO}^2 \phi_{2sC}^2 \phi_{2sO}^2 (\lambda_1 \phi_{CH_1}^2 - \lambda_2 \phi_{CH_1^*}^2) \times (\lambda_1 \phi_{CH_r}^2 - \lambda_2 \phi_{CH_r^*}^2 (\lambda_3 \phi_n^2 - \lambda_4 \phi_n^*^2) \times (\lambda_5 \phi_{CO\sigma}^2 - \lambda_6 \phi_{1\sigma^*}^2 - \lambda_7 \phi_{2\sigma^*}^2 - \lambda_8 \phi_{3\sigma^*}^2) \times (\lambda_9 \phi_{\pi}^2 - \lambda_{10} \phi_{1\pi^*}^2 - \lambda_{11} \phi_{2\pi^*}^2 - \lambda_{12} \phi_{3\pi^*}^2) \alpha \beta \alpha \beta \dots \alpha \beta \}$$

where we have labeled the *self-consistent* orbitals as to their qualitative nature. We see then that in the GVB(5/14/PP) wave function the CO  $\sigma$  and  $\pi$  bonds are each correlated with the three natural orbitals (the  $\sigma$  pair with two  $a_1$  orbitals and one  $b_2$  and the  $\pi$  pair with two  $b_1$ 's and one  $a_2$ ). In addition, the CH bonds and  $p_y$  lone pair are each correlated with one NO.

Similar calculations were carried out for the  $^2B_2$  ( $n \rightarrow \infty$ ) and  $^2B_1$  ( $\pi \rightarrow \infty$ ) ion states and for the  $^1B_1$  ( $n \rightarrow 3d_{xy}$ ) and  $^1B_2$  ( $\pi \rightarrow 3d_{xy}$ ) Rydberg states. The remaining Rydberg states were solved for using the Improved Virtual Orbital (IVO) method<sup>23,24</sup> with the self-consistent valence core orbitals from either the  $^1(n \rightarrow 3d_{xy})$  or the  $^1(\pi \rightarrow 3d_{xy})$  states.

Two sets of CI calculations<sup>25</sup> were carried out, one to describe states resulting from excitations out of the  $n$  orbital and the other to describe excitations out of the  $\pi$  orbital. The CI basis in each case consisted of the appropriate set of GVB(5/14/PP) orbitals plus the lowest nine IVO Rydberg orbitals from the appropriate IVO calculation.<sup>28</sup>

Table II. Summary of CI Calculations<sup>a</sup>

| States                 | Symmetry       | Valence dominant NO's |   |       | Rydberg orbitals |                |                |                | No. of spin eigenfunctions |         |
|------------------------|----------------|-----------------------|---|-------|------------------|----------------|----------------|----------------|----------------------------|---------|
|                        |                | $\sigma$ core         | n | $\pi$ | a <sub>1</sub>   | a <sub>2</sub> | b <sub>1</sub> | b <sub>2</sub> | Singlet                    | Triplet |
| G.S. (n)               | A <sub>1</sub> | N                     | A | N     |                  |                |                |                | 447                        |         |
| n → a <sub>1</sub>     | B <sub>2</sub> | N                     | A | N     | A                |                |                |                | 801                        | 1125    |
| n → a <sub>2</sub>     | B <sub>1</sub> | N                     | A | N     |                  | A              |                |                | 378                        | 546     |
| n → b <sub>1</sub>     | A <sub>2</sub> | N                     | A | N     |                  |                | A              |                | 725                        | 1040    |
| n → b <sub>2</sub>     | A <sub>1</sub> | N                     | A | N     |                  |                |                | A              | 560                        | 768     |
| n → ∞                  | B <sub>2</sub> | N                     | A | N     |                  |                |                |                |                            | 140     |
| G.S. ( $\pi$ )         | A <sub>1</sub> | N                     | N | A     |                  |                |                |                | 434                        |         |
| $\pi$ → a <sub>1</sub> | B <sub>1</sub> | N                     | N | A     | A                |                |                |                | 864                        | 1251    |
| $\pi$ → a <sub>2</sub> | B <sub>2</sub> | N                     | N | A     |                  | A              |                |                | 310                        | 460     |
| $\pi$ → b <sub>1</sub> | A <sub>1</sub> | N                     | N | A     |                  |                | A              |                | 680                        | 699     |
| $\pi$ → b <sub>2</sub> | A <sub>2</sub> | N                     | N | A     |                  |                |                | A              | 654                        | 936     |
| $\pi$ → ∞              | B <sub>1</sub> | N                     | N | A     |                  |                |                |                |                            | 123     |

<sup>a</sup> A = active set; N = inactive set; (blank) = not included in calculation.

In describing the configurations included in the CI calculations, it is convenient to define a set of active and inactive orbitals (see Table II). For the Rydberg states the active orbitals are defined to be those orbitals involved in the excitation. Thus, for example, the active orbitals in the (n → a<sub>1</sub> Rydberg) calculations are the n orbital and the a<sub>1</sub> Rydberg orbitals. Similarly, in the ion states the active set consists of the one singly occupied orbital. These definitions require two ground state calculations, one in which the active set is the n orbital (for comparison with n → Rydberg and n → ∞ states) and a second calculation in which the active set is the  $\pi$  orbital. In all cases the inactive set of orbitals is defined to be the remaining dominant NO's with the exception of the C1s and O1s orbitals which are not included in the CI calculations.

The CI calculations include all configurations resulting from at most a single excitation out of the inactive set together with up to a double excitation out of the active set (i.e., up to an overall triple excitation). The only other restrictions placed on the excitations are: (1) no excitations *between* the  $\sigma$  and  $\pi$  spaces are allowed, and (2) all configurations are restricted to have at most one electron in the Rydberg orbitals.

It has been found that this method of generating configurations includes the most important intrapair and interpair differential correlation effects necessary to describe *particular* ionizations or Rydberg excitations. It should be noted that this method neglects many important correlation effects involving the orbitals in the inactive set, but it is argued that correlations involving these orbitals will not lead to a significant differential effect. The basic assumption then is that in order to calculate, for example, the n ionization potential it is only necessary to include those correlations directly involving the n orbital.

### III. Results

**A. Rydberg Orbitals.** The Rydberg orbitals resulting from the IVO calculations are shown in Figures 1–3. Generally the orbitals are found, as expected, to resemble closely hydrogenic,  $n = 3$ , atomic orbitals.

Considering first the n-Rydberg states, Figure 1, we find most of the Rydberg orbitals to be centered approximately at the center of charge of the <sup>2</sup>B<sub>2</sub> ion (in the CH<sub>2</sub> region 0.016 Å from the carbon).<sup>29</sup> Deviations from this are more pronounced in the higher 3d states, in particular the 3d<sub>z<sup>2</sup>-x<sup>2</sup></sub> which is apparently centered in the CO region (see section IIID).

The orbital sizes, as indicated by  $\langle r^2 \rangle$  in Table III, are found to be highly dependent on the character, i.e., s, p, or d, of the orbital. For example, we find  $\langle 3s|r^2|3s \rangle = 44a_0^2$ ,  $\langle 3p|r^2|3p \rangle = 62 \pm 1a_0^2$ , and  $\langle 3d|r^2|3d \rangle = 115 \pm 2a_0^2$ , whereas, for comparison, the  $n = 3$  hydrogenic orbitals all lead to  $\langle r^2 \rangle =$

EXCITED STATE ORBITALS OF H<sub>2</sub>CO  
FROM EXCITATION OUT OF THE n ORBITAL

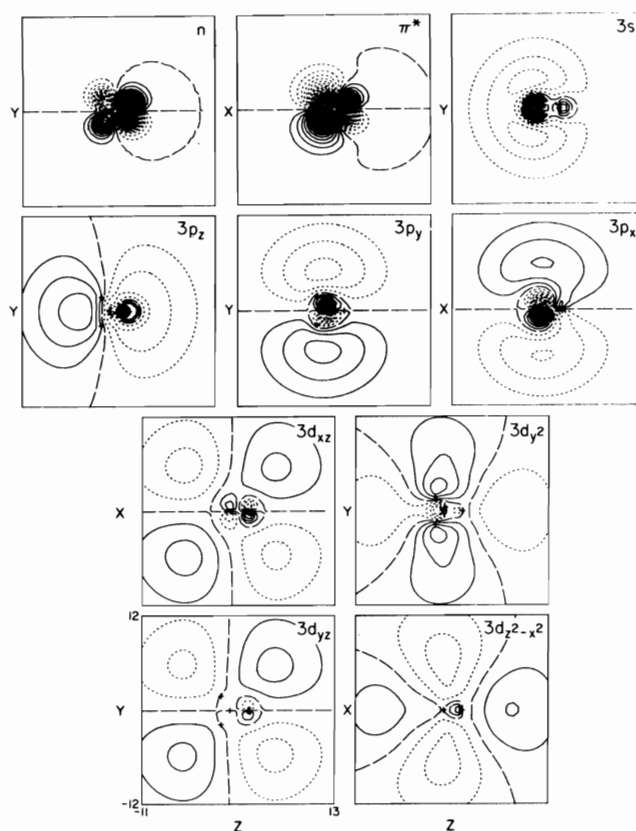


Figure 1. The Rydberg IVO's (singlet state) resulting from excitation out of the n orbital. The 3d<sub>xy</sub> is not shown. Long dashes indicate zero amplitude; the spacing between contours is 0.01 au. The same conventions are used in all plots. The molecule is in the yz plane.

126a<sub>0</sub><sup>2</sup>. Thus, as expected intuitively, the lower angular momentum Rydberg orbitals incorporate a greater degree of valence character than the higher angular momentum orbitals (for the same n).

The  $\pi$ -Rydberg IVO's shown in Figure 2 are found to resemble closely those of the n-Rydberg states (the center of charge of the  $\pi$  ion core is in the CH<sub>2</sub> region 0.12 Å from the carbon). The largest difference occurs in the 3d<sub>y<sup>2</sup></sub> orbital which has less density in the z direction than the n-Rydberg orbital.

**Table III.** Orbital  $x^2$ ,  $y^2$ ,  $z^2$  Expectation Values (Singlet States Unless Noted Otherwise)

|   | n $\rightarrow$ Rydberg states |       |       | $\pi \rightarrow$ Rydberg states <sup>a</sup> |                    |                    |
|---|--------------------------------|-------|-------|---|--------------------|--------------------|
|   | $x^2$                          | $y^2$ | $z^2$ | $x^2$   | $y^2$              | $z^2$              |
| 3s  | 14.09                          | 16.83 | 13.45 | 14.04   | 15.80              | 13.27              |
| 3p <sub>x</sub>                           | 36.18                          | 12.06 | 14.18 | 35.98 <sup>a</sup>                            | 11.99 <sup>a</sup> | 13.26 <sup>a</sup> |
| 3p <sub>y</sub>                           | 11.98                          | 36.01 | 12.90 | 11.97   | 36.01              | 12.84              |
| 3p <sub>z</sub>                           | 13.42                          | 13.82 | 35.57 | 14.78   | 14.18              | 34.82              |
| 3d <sub>y<sup>2</sup></sub>               | 37.32                          | 24.49 | 51.62 | 47.47   | 24.95              | 37.94              |
| 3d <sub>z<sup>2</sup>-x<sup>2</sup></sub> | 39.94                          | 29.76 | 47.18 | 28.29   | 30.38              | 61.11              |
| 3d <sub>xy</sub>                          | 49.99                          | 49.99 | 16.55 | 49.99   | 49.99              | 16.43              |
| 3d <sub>xz</sub>                          | 48.61                          | 16.20 | 48.32 | 47.73 <sup>a</sup>                            | 15.91 <sup>a</sup> | 47.23 <sup>a</sup> |
| 3d <sub>yz</sub>                          | 16.42                          | 49.27 | 49.00 | 16.29   | 48.89              | 48.00              |
| 2 $\pi$                                   |                                |       |       | 18.55   | 6.18               | 6.64               |
| 3 $\pi$                                   |                                |       |       | 28.45   | 9.48               | 17.69              |
| $\pi^*$                                   |                                |       |       | 3.12 <sup>a</sup>                             | 1.04 <sup>a</sup>  | 2.05 <sup>a</sup>  |

<sup>a</sup> These  $\pi^*$ , 3p<sub>x</sub>, and 3d<sub>xz</sub> orbitals are from transitions out of the  $\pi$  orbital with triplet pairing. (The 2 $\pi$  and 3 $\pi$  orbitals show the results for singlet pairing.)

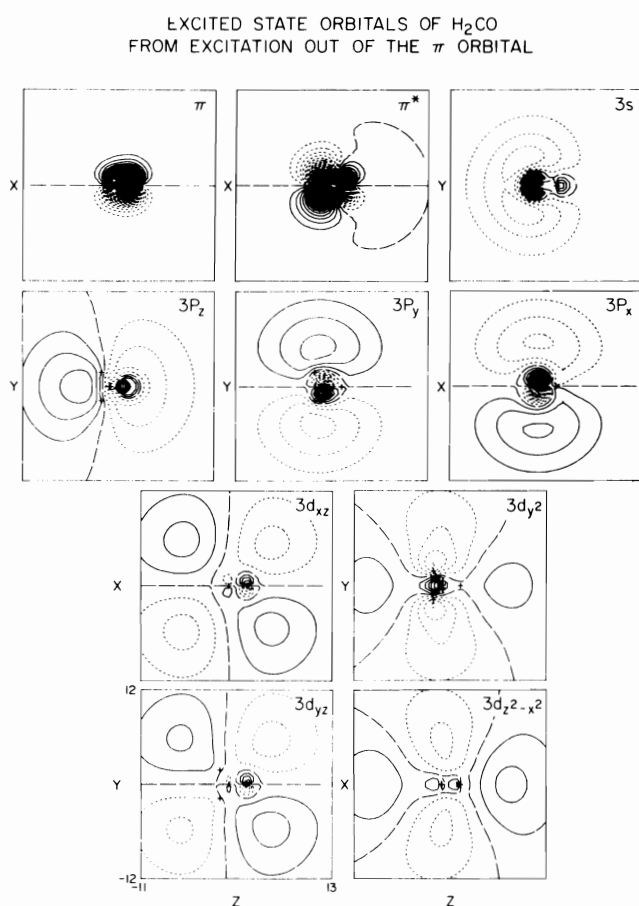


**Figure 2.** The Rydberg IVO's resulting from excitation out of the  $\pi$  orbital. The 3d<sub>xy</sub> is not shown. The  $\pi^*$ , 3p<sub>x</sub>, and 3d<sub>xz</sub> are taken from triplet state calculations (see Figure 3 for the singlet orbitals); the remainder are singlet state orbitals.

Of particular interest among the  $\pi$ -Rydberg states are the <sup>1</sup>A<sub>1</sub> states corresponding to <sup>1</sup>( $\pi \rightarrow 2\pi$ ) and <sup>1</sup>( $\pi \rightarrow 3\pi$ ). From Figure 3 we find the corresponding triplet states to consist of a valence <sup>3</sup>( $\pi \rightarrow \pi^*$ ) state and Rydberg <sup>3</sup>( $\pi \rightarrow 3p_x$ ) and <sup>3</sup>( $\pi \rightarrow 3d_{xz}$ ) states in which the Rydberg orbitals closely resemble the corresponding n  $\rightarrow$   $\pi$  Rydberg states. The singlet states, however, are found from IVO calculations to be very different, due to an apparent mixing of valence ( $\pi \rightarrow \pi^*$ ) character with Rydberg ( $\pi \rightarrow 3p_x$ ) character. The <sup>1</sup>( $\pi \rightarrow \pi^*$ ) state will be discussed in more detail in section IV.

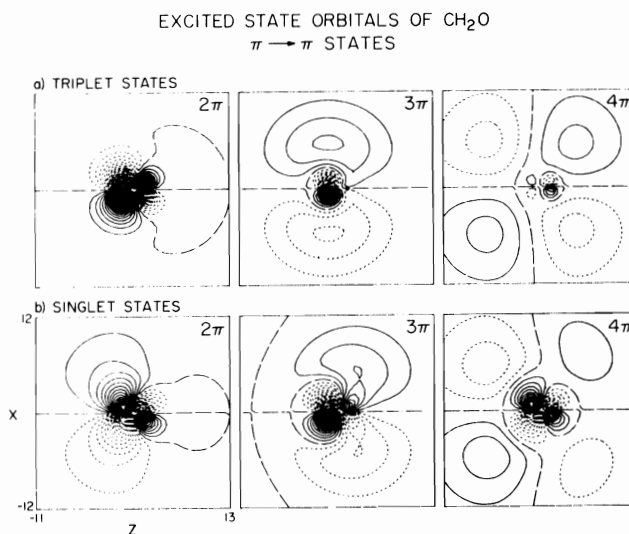


**Figure 3.** The valence and Rydberg IVO's resulting from  $\pi \rightarrow \pi$  singlet and triplet excitations.

**B. Excitation Energies.** The calculated excitation energies are listed in Tables IV and V together with the results of the theoretical calculations and experiments. The GVB-CI n  $\rightarrow$  Rydberg excitation energies (Table IV) are found to be within  $\sim 0.1$  eV of the experimental energies in those cases where accurate experimental numbers are available. Experimental results for the  $\pi \rightarrow$  Rydberg states are inconclusive due to a lack of resolution in the 10–13 eV range. However, broad peaks in the electron impact spectrum centered at 10.6, 11.7, and 12.8 eV correspond very closely to the calculated  $\pi \rightarrow 3s$ ,  $\pi \rightarrow 3p$ , and  $\pi \rightarrow 3d$  regions at 10.7, 11.8, and 12.8 eV, respectively. The lack of resolution in the spectrum and the small separation of individual 3p and 3d states makes assignments of particular transitions impossible.

The only accurate experimental excitation energies for  $\pi$ -Rydberg states are recent photoionization results<sup>30</sup> in which preionized states are observed at 11.46 and 12.48 eV. The first state has been assigned as <sup>1</sup>( $\pi \rightarrow 3p_z$ ), in good agreement with the GVB-CI result (11.66 eV). The second state was assigned as <sup>1</sup>( $\pi \rightarrow 4s$ ), although the GVB-CI results indicate it may be a <sup>1</sup>( $\pi \rightarrow 3d$ ) state (Table V).

Also of interest is a direct test of the reliability of the Improved Virtual Orbital method. IVO calculations rely on the assumption that the valence core of a given Rydberg state is

Table IV. Vertical Excitation Energies (eV) for CH<sub>2</sub>O: n<sup>1</sup> States

| Character                                     | State                       | Experimental         |                       | Present work        |                  | Other theoretical work |                    |                  |                  |
|---|-----------------------------|----------------------|-----------------------|---------------------|------------------|------------------------|--------------------|------------------|------------------|
|   |                             | Optical <sup>a</sup> | e impact <sup>b</sup> | GVB-CI <sup>c</sup> | IVO <sup>d</sup> | HF <sup>e</sup>        | HF-CI <sup>e</sup> | RPA <sup>f</sup> | EOM <sup>g</sup> |
| n → π*  | <sup>3</sup> A <sub>2</sub> |                      | 3.5                   | 3.68                |                  | 2.25                   | 3.41               | 2.15             | 3.46             |
|   | <sup>1</sup> A <sub>2</sub> |                      | 4.1                   | 4.09                | 5.51             | 2.62                   | 3.81               | 3.47             | 4.04             |
| n → 3s  | <sup>3</sup> B <sub>2</sub> |                      | 7.09                  | 7.08                |                  | 6.03                   | 7.32               |                  |                  |
|   | <sup>1</sup> B <sub>2</sub> | 7.091                | 7.13                  | 7.16                | 7.56             | 6.07                   | 7.38               |                  | 7.28             |
| n → 3p <sub>z</sub>                           | <sup>3</sup> B <sub>2</sub> |                      | 7.92                  | 7.99                |                  |                        | 8.29               |                  |                  |
|   | <sup>1</sup> B <sub>2</sub> | 7.97                 | 8.00                  | 8.08                | 8.40             |                        | 8.39               |                  | 8.12             |
| n → 3p <sub>y</sub>                           | <sup>3</sup> A <sub>1</sub> |                      | 8.11                  | 8.05                |                  | 6.93                   | 8.09               |                  |                  |
| n → 3p <sub>x</sub>                           | <sup>1</sup> A <sub>1</sub> | 8.14                 | 8.15                  | 8.09                | 8.42             |                        | 8.11               |                  | 8.15             |
|   | <sup>3</sup> A <sub>2</sub> |                      | (8.31)                | 8.31                |                  |                        | 9.06               |                  |                  |
| n → 3d <sub>y<sup>2</sup></sub>               | <sup>1</sup> A <sub>2</sub> |                      |                       | 8.32                | 8.71             |                        | 9.07               |                  | 8.35             |
|   | <sup>3</sup> B <sub>2</sub> |                      |                       | 9.01                |                  |                        |                    |                  |                  |
| n → 3d <sub>z<sup>2</sup>-x<sup>2</sup></sub> | <sup>1</sup> B <sub>2</sub> | 8.88                 | 8.92                  | 9.05                | 9.35             |                        |                    |                  |                  |
|   | <sup>3</sup> B <sub>2</sub> |                      |                       | 9.16                |                  |                        |                    |                  |                  |
| n → 3d <sub>xy</sub>                          | <sup>1</sup> B <sub>2</sub> |                      |                       | 9.17                | 9.45             |                        |                    |                  |                  |
|   | <sup>3</sup> B <sub>1</sub> |                      |                       | 9.21                |                  |                        |                    |                  |                  |
| n → 3d <sub>xz</sub>                          | <sup>1</sup> B <sub>1</sub> |                      |                       | 9.21                | 9.47             |                        |                    |                  |                  |
|   | <sup>3</sup> A <sub>2</sub> |                      |                       | 9.23                |                  |                        |                    |                  |                  |
| n → 3d <sub>yz</sub>                          | <sup>1</sup> A <sub>2</sub> |                      |                       | 9.24                | 9.53             |                        |                    |                  |                  |
|   | <sup>3</sup> A <sub>1</sub> |                      |                       | 9.17                |                  |                        |                    |                  |                  |
| n → ∞   | <sup>1</sup> A <sub>1</sub> | 9.03                 | 9.07                  | 9.23                | 9.50             |                        |                    |                  |                  |
|   | <sup>2</sup> B <sub>2</sub> | 10.87                | 10.87                 | 10.55               |                  | 9.47                   |                    |                  |                  |

<sup>a</sup> Reference 9. <sup>b</sup> Our assignment of unpublished spectra by A. Chutjian. <sup>c</sup> Ground state  $E = -113.95686$ . <sup>d</sup> Experimental ionization potential minus IVO orbital eigenvalue. <sup>e</sup> Reference 10. <sup>f</sup> T. H. Dunning, Jr., and V. McKoy, *J. Chem. Phys.*, **48**, 5263 (1968). <sup>g</sup> Reference 14.

Table V. Vertical Excitation Energies (eV) for CH<sub>2</sub>O: π<sup>1</sup> States

| Character                                     | State                       | Exptl<br>e impact <sup>a</sup> | Present work        |                  | Other theoretical work |                    |                  |                  |
|---|-----------------------------|--------------------------------|---------------------|------------------|------------------------|--------------------|------------------|------------------|
|   |                             |                                | GVB-CI <sup>b</sup> | IVO <sup>c</sup> | HF <sup>d</sup>        | HF-CI <sup>d</sup> | RPA <sup>e</sup> | EOM <sup>f</sup> |
| π → π*  | <sup>3</sup> A <sub>1</sub> | 6.0                            | 5.95 <sup>g</sup>   | 7.56             | 4.17                   | 5.56               |                  | 5.29             |
|   | <sup>1</sup> A <sub>1</sub> | 10.7                           | 10.77               | 11.30            |                        | 11.41              | 11.22            | 10.30            |
| π → 3s  | <sup>3</sup> B <sub>1</sub> |                                | 10.68               |                  |                        |                    |                  |                  |
|   | <sup>1</sup> B <sub>1</sub> | 10.7                           | 10.73               | 11.02            |                        |                    |                  | 11.2             |
| π → 3p <sub>z</sub>                           | <sup>3</sup> B <sub>1</sub> |                                | 11.57               |                  |                        |                    |                  |                  |
|   | <sup>1</sup> B <sub>1</sub> | 11.6-11.9                      | 11.66               | 11.96            |                        |                    |                  | 12.2             |
| π → 3p <sub>y</sub>                           | <sup>3</sup> A <sub>2</sub> |                                | 11.63               |                  |                        |                    |                  |                  |
|   | <sup>1</sup> A <sub>2</sub> |                                | 11.78               | 11.93            |                        |                    |                  |                  |
| π → 3p <sub>x</sub>                           | <sup>3</sup> A <sub>1</sub> |                                | 11.77               | 12.08            |                        |                    |                  |                  |
|   | <sup>1</sup> A <sub>1</sub> | 11.6-11.9                      | 12.00               | 12.58            |                        |                    |                  |                  |
| π → 3d <sub>y<sup>2</sup></sub>               | <sup>3</sup> B <sub>1</sub> |                                | 12.57               |                  |                        |                    |                  |                  |
|   | <sup>1</sup> B <sub>1</sub> | 12.5-12.8                      | 12.58               | 12.86            |                        |                    |                  |                  |
| π → 3d <sub>z<sup>2</sup>-x<sup>2</sup></sub> | <sup>3</sup> B <sub>1</sub> |                                | 12.68               |                  |                        |                    |                  |                  |
|   | <sup>1</sup> B <sub>1</sub> | 12.5-12.8                      | 12.70               | 12.96            |                        |                    |                  |                  |
| π → 3d <sub>xy</sub>                          | <sup>3</sup> B <sub>2</sub> |                                | 12.75               | 12.98            |                        |                    |                  |                  |
|   | <sup>1</sup> B <sub>2</sub> | 12.5-12.8                      | 12.75               | 12.98            |                        |                    |                  |                  |
| π → 3d <sub>xz</sub>                          | <sup>3</sup> A <sub>1</sub> |                                | 12.76               | 13.02            |                        |                    |                  |                  |
| π → 3d <sub>yz</sub>                          | <sup>3</sup> A <sub>2</sub> |                                | 12.74               |                  |                        |                    |                  |                  |
|   | <sup>1</sup> A <sub>2</sub> |                                | 12.88               | 13.02            |                        |                    |                  |                  |
| π → ∞   | <sup>2</sup> B <sub>1</sub> | 14.4                           | 14.14               |                  |                        |                    |                  |                  |

<sup>a</sup> Our assignment of unpublished spectra by A. Chutjian. <sup>b</sup> Ground state  $E = -113.98763$ . <sup>c</sup> Experimental ionization potential minus IVO orbital eigenvalue. <sup>d</sup> Reference 10. <sup>e</sup> T. H. Dunning, Jr., and V. McKoy, *J. Chem. Phys.*, **48**, 5263 (1968). <sup>f</sup> Reference 14. <sup>g</sup> This value is GVB-CI using GVB orbitals for the triplet state. Use of the IVO orbitals plus ground state GVB orbitals as in the rest of the states in this table leads to  $\Delta E = 8.08$  eV.

not greatly affected by the precise nature of the diffuse orbital. In addition, IVO calculations assume the correlation energies of the Rydberg states are all approximately equal to those of the corresponding ion states. The results in Tables IV and V indicate that IVO excitation energies are generally 0.3 to 0.4 eV above the more accurate GVB-CI results. We do find the error in the IVO excitations to be fairly constant with the exception of the <sup>1</sup>(π → π\*) state, and hence accurate predictions (±0.1 eV) based on corrected IVO excitation energies are possible.

**C. Oscillator Strengths.** The oscillator strengths calculated from GVB-CI wave functions are in poor agreement with experimental results (Table VI). The GVB-CI <sup>1</sup>(n → 3s) oscillator strength is approximately a factor of 4 too small. Similar errors are found in all the allowed <sup>1</sup>(n → 3d) transitions.

The GVB-CI <sup>1</sup>(n → 3p) oscillator strengths, however, are in good agreement with experiment, the calculated results being ~20% below the experimental results. The (n → 3p<sub>y</sub>) absorption is calculated to be approximately twice as intense

Table VI. Oscillator Strengths for CH<sub>2</sub>O

| State                          | $f_{\text{calcd}}$<br>No. 1 | $f_{\text{calcd}}^a$<br>No. 2 | $f_{\text{obsd}}^b$ |
|--------------------------------|-----------------------------|-------------------------------|---------------------|
| $n \rightarrow 3s$             | 0.006                       | 0.007                         | 0.038               |
| $n \rightarrow 3p_z$           | 0.015                       | 0.014                         | 0.017               |
| $n \rightarrow 3p_y$           | 0.030                       | 0.031                         | 0.038               |
| $n \rightarrow 3d_{y^2}$       | 0.005                       | 0.007                         | 0.010               |
| $n \rightarrow 3d_{z^2-x^2}$   | 0.0004                      | ~0.0                          |                     |
| $n \rightarrow 3d_{yz}$        | 0.0002                      | 0.0005                        | 0.012               |
| $n \rightarrow 3d_{xy}$        | 0.0001                      | 0.0002                        |                     |
| $\pi \rightarrow 3s$           | 0.026                       |                               |                     |
| $\pi \rightarrow 1\pi^*$       | 0.256                       | 0.255                         |                     |
| $\pi \rightarrow 2\pi^*$       | 0.036                       |                               |                     |
| $\pi \rightarrow 3p_z$         | 0.026                       |                               |                     |
| $\pi \rightarrow 3d_{y^2}$     | 0.0001                      |                               |                     |
| $\pi \rightarrow 3d_{z^2-x^2}$ | 0.015                       |                               |                     |
| $\pi \rightarrow 3d_{xy}$      |                             |                               |                     |

<sup>a</sup> The results of a more accurate calculation using two sets of diffuse d functions. <sup>b</sup> Reference 9.

Table VII. GVB-Cl Dipole Moments for CH<sub>2</sub>O (Ground State Geometry, GVB-Cl)<sup>a</sup>

|   | au                  | Debye              |
|---|---------------------|--------------------|
| G.S.  | -0.93 <sup>b</sup>  | -2.36 <sup>b</sup> |
| <sup>3</sup> ( $n \rightarrow \pi^*$ )          | -0.600 <sup>b</sup> | -1.52              |
| <sup>1</sup> ( $n \rightarrow \pi^*$ )          | -0.665 <sup>b</sup> | -1.69              |
| <sup>1</sup> ( $n \rightarrow 3s$ )             | +1.207              | 3.068              |
| <sup>1</sup> ( $n \rightarrow 3p_z$ )           | -0.718              | -1.825             |
| <sup>1</sup> ( $n \rightarrow 3p_y$ )           | +0.151              | 0.384              |
| <sup>1</sup> ( $n \rightarrow 3p_x$ )           | -0.149              | -0.379             |
| <sup>1</sup> ( $n \rightarrow 3d_{y^2}$ )       | -1.172              | -2.979             |
| <sup>1</sup> ( $n \rightarrow 3d_{z^2-x^2}$ )   | -2.441              | -6.204             |
| <sup>1</sup> ( $n \rightarrow 3d_{xy}$ )        | -0.014              | -0.036             |
| <sup>1</sup> ( $n \rightarrow 3d_{xz}$ )        | -0.161              | -0.409             |
| <sup>1</sup> ( $n \rightarrow 3d_{yz}$ )        | -0.433              | -1.101             |
| <sup>3</sup> ( $\pi \rightarrow \pi^*$ )        | -0.523 <sup>b</sup> | -1.33              |
| <sup>1</sup> ( $\pi \rightarrow 3s$ )           | 1.175               | 2.986              |
| <sup>1</sup> ( $\pi \rightarrow \pi^*$ )        | -0.130              | -0.330             |
| <sup>1</sup> ( $\pi \rightarrow 3p_z$ )         | -0.749              | -1.904             |
| <sup>1</sup> ( $\pi \rightarrow 3p_y$ )         | 0.264               | +0.671             |
| <sup>3</sup> ( $\pi \rightarrow 3p_x$ )         | -0.259              | -0.658             |
| <sup>1</sup> ( $\pi \rightarrow 3p_x$ )         | -2.350              | -5.973             |
| <sup>1</sup> ( $\pi \rightarrow 3d_{y^2}$ )     | 0.123               | 0.313              |
| <sup>1</sup> ( $\pi \rightarrow 3d_{z^2-x^2}$ ) | -2.261              | -5.747             |
| <sup>1</sup> ( $\pi \rightarrow 3d_{xy}$ )      | +0.075              | 0.191              |
| <sup>3</sup> ( $\pi \rightarrow 3d_{xz}$ )      | +0.455              | 1.156              |
| <sup>1</sup> ( $\pi \rightarrow 3d_{yz}$ )      | -0.104              | -0.264             |

<sup>a</sup> Positive sign indicates electrons moved from O end to H end.  
<sup>b</sup> From ref 2.

as the ( $n \rightarrow 3p_z$ ). This ordering is in agreement with the results of the equations of motion calculations although those calculations led to a considerably smaller difference. These results contradict the reported assignment<sup>8,9</sup> of the ( $n \rightarrow 3p$ ) states in which the more intense absorption is assumed to be the <sup>1</sup>( $n \rightarrow 3p_z$ ) state.

In order to test possible insufficiency of the diffuse d basis, a second set of calculations was carried out employing a more flexible d basis (see section II). These calculations resulted in no significant improvement in the accuracy of the oscillator strength results (Table VI).

**D. Dipole Moments.** The GVB-Cl dipole moments of the Rydberg states of formaldehyde are listed in Table VII. There are no experimental results for comparison; however, GVB-Cl dipole moments for the ground and valence excited states were found to be in excellent agreement with experiment.<sup>2</sup>

Assuming the valence core of each Rydberg series to be independent of the particular Rydberg state, the variations in the dipole moments of these states can be interpreted as shifts in the center of charge of the Rydberg orbitals. In addition, if the Rydberg orbital were centered (symmetrically) at the center of charge of the valence core, the net dipole moment would be zero. Therefore, deviations from zero may be interpreted as shifts of the Rydberg orbitals relative to the core center of charge.

Considering first the  $n$ -Rydberg states we find the lowest energy orbitals of  $a_1$  and  $b_2$  symmetry,  $3s$  and  $3p_y$ , respectively, are shifted toward the hydrogen while the higher orbitals of these symmetries are shifted toward the oxygen. All of the Rydberg orbitals of  $b_1$  and  $a_2$  symmetry, however, are shifted slightly toward the oxygen.

A similar effect is found in the  $a_1$  and  $b_2$   $\pi$ -Rydberg orbitals with the exception of the  $3d_{x^2}$  which is found to be shifted in the same direction as the  $3s$  (toward the hydrogens). The  $b_1$  and  $a_2$   $\pi$ -Rydberg orbitals are found to be shifted to a much greater extent than the corresponding  $n$ -Rydberg orbitals. This is probably due to larger exchange interactions with the singly occupied core orbital ( $\pi$  in this case).

The observed shifts in the sigma Rydberg orbitals can be explained by considering the polarity of the CH bonds. Mulliken population analysis leads to net core charges on each hydrogen of 0.33 (<sup>2</sup>B<sub>2</sub>) and +0.29 (<sup>2</sup>B<sub>1</sub>). Thus the lowest Rydberg orbital of each  $\sigma$  symmetry is stabilized by a shift toward the hydrogen while the higher orbitals, due to orthogonality constraints, are shifted in the opposite direction.

#### IV. Discussion

There has been some controversy in the literature concerning the character and location of the <sup>1</sup>( $\pi \rightarrow \pi^*$ ) state of formaldehyde and other simple  $\pi$ -bonded molecules. In light of this we include here a brief summary of the results of previous calculations on this state of formaldehyde, an analysis of the results of the GVB-Cl calculations, and a discussion of the discrepancies between the GVB-Cl results and those of other calculations.

The earliest calculations on the <sup>1</sup>( $\pi \rightarrow \pi^*$ ) state of CH<sub>2</sub>O were semiempirical, PPP calculations.<sup>31</sup> These calculations assumed the state to be valence and predicted an excitation energy of 7.4 eV. Buenker and Peyerimhoff,<sup>31</sup> in an ab initio CI calculation without diffuse basis functions, found the <sup>1</sup>( $\pi \rightarrow \pi^*$ ) state to be 11.71 eV above the ground state. Later they<sup>10</sup> and Whitten and Hackmeyer<sup>11</sup> reported that addition of diffuse functions to the basis set leads to a *Rydberg-like* <sup>1</sup>( $\pi \rightarrow \pi^*$ ) state with an excitation energy of 11.3 to 11.4 eV. In more extensive calculations including  $\sigma$ - $\pi$  correlations and d polarization functions, Whitten<sup>13</sup> concluded the state to be *valence-like* with an excitation energy of 9.9 eV. More recently, Yeager and McKoy<sup>14</sup> have reported equations of motion calculations that lead to a semi-Rydberg <sup>1</sup>( $\pi \rightarrow \pi^*$ ) state located at 10.31 eV. Finally, Langhoff et al.<sup>15</sup> have studied the <sup>1</sup>( $\pi \rightarrow \pi^*$ ) state with MC-SCF and CI wave functions. They conclude the state to be *valence* in character with an excitation energy of 11.2 eV.

Our single configuration IVO calculations lead to a fairly diffuse state with  $\langle \pi^* | r^2 | \pi^* \rangle$  being approximately five times that of the triplet  $\pi^*$ , Table III. Considering the overlaps of the singlet and triplet IVO orbitals, Table VIII, we find the single configuration <sup>1</sup>( $\pi \rightarrow \pi^*$ ) state to be approximately 66% valence in character and 34% Rydberg. This is a slight overestimate of the valence character of the singlet IVO since the IVO triplet  $\pi^*$  orbital is more diffuse than the self-consistent orbital (the IVO approximation is not as accurate for valence states). Using the self-consistent triplet orbital leads to the conclusion of 50% valence character in the <sup>1</sup>( $\pi \rightarrow \pi^*$ ) state.



**Table VIII.** Overlaps of Singlet and Triplet ( $\pi \rightarrow \pi^*$ ) IVO Orbitals

|                        | Triplet state orbitals |               |                  |       |
|------------------------|------------------------|---------------|------------------|-------|
|                        | $2\pi (\pi^*)$         | $3\pi (3p_x)$ | $4\pi (3d_{xz})$ | Other |
| Singlet state orbitals |                        |               |                  |       |
| $2\pi$                 | 0.812                  | 0.534         | -0.171           | 0.162 |
| $3\pi$                 | 0.429                  | -0.808        | -0.384           | 0.125 |
| $4\pi$                 | -0.319                 | 0.240         | -0.903           | 0.288 |
| Other                  | 0.234                  | 0.066         | 0.089            |       |

In the CI calculations the  $^1(\pi \rightarrow \pi^*)$  state is found to contract considerably leading to an effective  $\langle \pi^* | r^2 | \pi^* \rangle^{33}$  less than half that of the IVO result. This contraction results from a CI mixing of the single configuration  $^1(1\pi \rightarrow 2\pi)$  state with the  $^1(1\pi \rightarrow 3\pi)$  state. The net effect is a decrease in  $\langle 2\pi | x^2 | 2\pi \rangle$  from an IVO value of  $18.55a_0$  to an effective CI value of  $8.34a_0$  with a corresponding increase in  $\langle 3\pi | x^2 | 3\pi \rangle$  from  $28.45a_0$  to  $40.16a_0$ . In comparison a purely valence  $\pi^*$  orbital would have an  $\langle x^2 \rangle$  of  $3.1a_0^2$  whereas a purely Rydberg  $\pi^*$  orbital would have an  $\langle x^2 \rangle$  of  $48.6a_0^2$  (see Table III). Thus we conclude that the  $^1(\pi \rightarrow \pi^*)$  state of formaldehyde is essentially ( $\sim 90\%$ ) valence in character.

The GVB-CI  $^1(\pi \rightarrow \pi^*)$  excitation energy, 10.77 eV, is much lower than expected for either a Rydberg  $3p_x$  state ( $\sim 11.8$  eV) or a purely valence state analogous to the  $^3(\pi \rightarrow \pi^*)$  state [ $E(\text{triplet}) + 2K_{\pi\pi^*} = 12.5$  eV]. It is also noted that the single configuration IVO treatment of this state is clearly anomalous. For all the pure  $\pi$ -Rydberg states the IVO excitation energy is consistently 0.2 to 0.3 eV above the GVB-CI result. However, the IVO  $^1(\pi \rightarrow \pi^*)$  excitation energy is 0.53 eV above the CI energy. This is consistent with the conclusion of a large CI mixing of the  $^1(1\pi \rightarrow 2\pi)$  and  $^1(1\pi \rightarrow 3\pi)$  IVO states.

Experimental evidence concerning the location of the  $^1(\pi \rightarrow \pi^*)$  state is inconclusive. Recent electron impact spectra<sup>5,6</sup> show a broad peak from 10.4 to 11.0 eV with a maximum at  $\sim 10.7$  eV. The vibrational progression in this peak, although poorly resolved, is consistent with a C-O stretching frequency of approximately  $1130 \text{ cm}^{-1}$  (the stretching frequency of the  $^2B_1$  ion is reported<sup>34</sup> to be  $1210 \text{ cm}^{-1}$ ). Thus these results are consistent with a  $^1(\pi \rightarrow \pi^*)$  state located at  $\sim 10.7$  eV. This assignment is complicated by the GVB-CI prediction of a second, more weakly absorbing state,  $^1(\pi \rightarrow 3s)$ , in this region.

Whitten<sup>13</sup> has argued that d-polarization functions and  $\sigma$  correlation are necessary for an accurate description of the  $^1(\pi \rightarrow \pi^*)$  state. The calculations reported here include both of these effects and yet lead to results that differ significantly from those of Whitten. Whitten's conclusions are based primarily on two CI calculations. In the first CI calculation only configurations of the form a-d (Chart I) were included. In the

**Chart I**

|   | $\sigma_k$ | $\sigma_k^*$ | $\pi$ | $\pi^*$ |
|---|------------|--------------|-------|---------|
| a | 2          | 0            | 2     | 0       |
| b | 2          | 0            | 0     | 2       |
| c | 1          | 1            | 2     | 0       |
| d | 1          | 1            | 0     | 2       |
| e | 1          | 1            | 1     | 1       |

calculations reported here all configurations resulting from single  $\sigma$  excitations with any order  $\pi$  excitation were included. It was found that configurations of the form (e), representing  $\sigma$ - $\pi$  interpair correlation effects, are very important in the ground state wave function. These configurations account for

approximately 1.1 eV of the CI energy lowering. Therefore calculations in which these configurations are excluded are expected to lead to erroneously low excitation energies. In the second of Whitten's CI calculations the  $\sigma^*$  orbitals were chosen primarily to describe readjustments resulting from a highly polarized  $\pi$  system, one with either a doubly occupied oxygen p orbital or a doubly occupied carbon p orbital. It is certainly the case that this choice strongly favors the  $^1(\pi \rightarrow \pi^*)$  state over the ground state and hence this calculation should also lead to an anomalously low excitation energy.

A second point that has been discussed at length in the literature is the possibility of mixing occurring between the  $^1(\pi \rightarrow \pi^*)$  state and the lower lying ( $n \rightarrow p_y$ ) and ( $n \rightarrow d_{yz}$ ) states of the same symmetry. The only reported calculations on the extent of this mixing are those of Mentall et al.<sup>9</sup> These calculations assume the  $^1(\pi \rightarrow \pi^*)$  state to be purely valence in character and hence are expected to overestimate greatly the amount of mixing. In our calculations the  $^1(\pi \rightarrow \pi^*)$  state is not allowed to interact with the Rydberg  $^1(n \rightarrow 3p_y)$  or  $^1(n \rightarrow 3d_{yz})$  states. However, the  $^1(\pi \rightarrow \pi^*)$  state is allowed to interact with a valence  $^1(n \rightarrow 2p_y^*)$  "state" and, in fact, the resulting wave function is found to have  $\sim 1\%$  ( $n \rightarrow 2p_y^*$ ) character. We, however, interpret this CI effect as an  $n$ - $\pi$  interpair correlation.

## References and Notes

- (1) Partially supported by a grant (CHE74-05132) from the National Science Foundation.
- (2) L. B. Harding and W. A. Goddard III, *J. Am. Chem. Soc.*, **97**, 6293 (1975).
- (3) E. P. Gientieu and J. E. Mentall, *Science*, **169**, 681 (1970).
- (4) A. Chutjian, *J. Chem. Phys.*, **61**, 4279 (1974).
- (5) A. Chutjian, unpublished results.
- (6) M. J. Weiss, C. E. Kuyatt, and S. Mielczanek, *J. Chem. Phys.*, **54**, 4147 (1971).
- (7) D. C. Moule and A. D. Walsh, *Chem. Rev.*, **75**, 67 (1975).
- (8) C. R. Lassar, D. C. Moule, and S. Bell, *Chem. Phys. Lett.*, **29**, 603 (1974).
- (9) J. E. Mentall, E. P. Gientieu, M. Krauss, and D. Neumann, *J. Chem. Phys.*, **55**, 5471 (1971).
- (10) S. D. Peyerimhoff, R. J. Buenker, W. E. Krammer, and H. Hsu, *Chem. Phys. Lett.*, **8**, 129 (1971).
- (11) J. L. Whitten and M. Hackmeyer, *J. Chem. Phys.*, **51**, 5584 (1969).
- (12) K. Tanaka, *Int. J. Quantum Chem.*, **8**, 981 (1974).
- (13) J. L. Whitten, *J. Chem. Phys.*, **56**, 5458 (1972).
- (14) D. L. Yeager and V. McKoy, *J. Chem. Phys.*, **60**, 2714 (1974).
- (15) S. R. Langhoff, S. T. Elbert, C. F. Jackels, and E. R. Davidson, *Chem. Phys. Lett.*, **29**, 247 (1974).
- (16) S. Huzinaga, *J. Chem. Phys.*, **42**, 1293 (1965).
- (17) T. H. Dunning, Jr., *J. Chem. Phys.*, **53**, 2823 (1970).
- (18) T. H. Dunning, Jr., unpublished results.
- (19) R. B. Lawrence and M. W. P. Strandberg, *Phys. Rev.*, **83**, 363 (1951).
- (20) W. J. Hunt, P. J. Hay, and W. A. Goddard III, *J. Chem. Phys.*, **57**, 738 (1972).
- (21) The GVB(PP) calculations were carried out with the Bobrowicz-Wadt-Yaffe-Goddard program (GVB-TWO) using the basic methods of ref 20.
- (22) L. B. Harding and W. A. Goddard III, unpublished results.
- (23) W. J. Hunt and W. A. Goddard III, *Chem. Phys. Lett.*, **3**, 414 (1969).
- (24) W. A. Goddard III and W. J. Hunt, *Chem. Phys. Lett.*, **24**, 464 (1974).
- (25) The CI calculations were carried out with the Caltech Spin Eigenfunction CI program (Bobrowicz, Winter, Ladner, Moss, Harding, and Goddard),<sup>26,27</sup>
- (26) F. W. Bobrowicz, Ph.D. Thesis, California Institute of Technology, 1974.
- (27) R. C. Ladner, Ph.D. Thesis, California Institute of Technology, 1971.
- (28) For states involving, for example, excitation out of the  $\pi$  orbital,  $\pi$ -correlating orbitals were taken from the ground state calculation.
- (29) The reader may be surprised that the ion resulting from excitation out of the oxygen n orbital has a center of charge in the  $\text{CH}_2$  region. However, as a result of the polarity of the ground state wave function, removal of an electron in the ground state  $2b_2$  orbital (with no orbital readjustments) leads to a center of charge 0.035 Å away from the carbon (toward the oxygen). Orbital readjustments (SCF) in the ion then account for the remaining shift of 0.051 Å further away from the oxygen.
- (30) P. M. Guyon, W. A. Chupka, and J. Berkowitz, *J. Chem. Phys.*, **64**, 1419 (1976).
- (31) T. Anno and A. Sado, *J. Chem. Phys.*, **26**, 1759 (1957).
- (32) R. J. Buenker and S. D. Peyerimhoff, *J. Chem. Phys.*, **53**, 1368 (1970).
- (33) We define the effective CI  $\langle \pi^* | r^2 | \pi^* \rangle$  to be  $\langle \psi_2 | r^2 | \psi_2 \rangle - \langle \psi_1 | r^2 | \psi_1 \rangle + \langle \pi | r^2 | \pi \rangle$  where  $\psi_2$  is the  $^1(\pi \rightarrow \pi^*)$  CI wave function,  $\psi_1$  is the ground state CI wave function using the orbitals of the  $^1(\pi \rightarrow \pi^*)$  CI calculation, and  $\pi$  is the ground state  $\pi$  orbital.
- (34) D. W. Turner, "Molecular Photoelectron Spectroscopy", Wiley, New York, N.Y., 1970.